HHS Public Access

Author manuscript

Genesis. Author manuscript; available in PMC 2018 March 01.

Published in final edited form as:

Genesis. 2017 March ; 55(3): . doi:10.1002/dvg.23021.

Nkx2.5 regulates Endothelin Converting Enzyme-1 during pharyngeal arch patterning

Jennifer M. Iklé[1], **Andre L. P. Tavares**[1], **Marisol King**[1], **Hailei Ding**[1,*], **Sophie Colombo**[2], **Beth A. Firulli**[3], **Anthony B. Firulli**[3], **Kimara L. Targoff**[2], **Deborah Yelon**[4], and **David E. Clouthier**[1,§]

[1]Department of Craniofacial Biology, University of Colorado Anschutz Medical Campus, Aurora, CO 80045, USA

[2]Division of Cardiology, Department of Pediatrics, College of Physicians and Surgeons, Columbia University, New York, NY 10032, USA

[3]Riley Heart Research Center, Herman B Wells Center for Pediatric Research, Division of Pediatric Cardiology, Departments of Anatomy and Medical, Biochemistry, and Molecular Genetics, Indiana Medical School, Indianapolis, IN 46202, USA

[4]Division of Biological Sciences, University of California, San Diego, La Jolla, CA 92093, USA

Abstract

In gnathostomes, dorsoventral (D-V) patterning of neural crest cells (NCC) within the pharyngeal arches is crucial for the development of hinged jaws. One of the key signals that mediates this process is Endothelin-1 (EDN1). Loss of EDN1 binding to the Endothelin-A receptor (EDNRA) results in loss of EDNRA signaling and subsequent facial birth defects in humans, mice and zebrafish. A rate-limiting step in this crucial signaling pathway is the conversion of immature EDN1 into a mature active form by Endothelin converting enzyme-1 (ECE1). However, surprisingly little is known about how *Ece1* transcription is induced or regulated. We show here that Nkx2.5 is required for proper craniofacial development in zebrafish and acts in part by upregulating *ece1* expression. Disruption of *nkx2.5* in zebrafish embryos results in defects in both ventral and dorsal pharyngeal arch-derived elements, with changes in ventral arch gene expression consistent with a disruption in Ednra signaling. *ece1* mRNA rescues the *nkx2.5* morphant phenotype, indicating that Nkx2.5 functions through modulating Ece1 expression or function. These studies illustrate a new function for Nkx2.5 in embryonic development and provide new avenues with which to pursue potential mechanisms underlying human facial disorders.

Keywords

Birth defects; Patterning; Transcription; Signaling; Neural crest

[§]Correspondence address: David E. Clouthier. Ph.D., Department of Craniofacial Biology, University of Colorado Anschutz Medical Campus, Aurora, CO 80045, USA, Phone: 011-303-724-4565, FAX: 011-303-724-4580, david.clouthier@ucdenver.edu.

[*]Current addresses: Jiangsu Province Key Laboratory of Anesthesiology and Jiangsu Province Key Laboratory of Anesthesia Application Technology, Xuzhou Medical University, Xuzhou 221004, Jiangsu Province, China.

INTRODUCTION

A diverse set of instructive signals drive dorsoventral patterning of cranial neural crest cells (NCCs) that will eventually form the craniofacial skeleton (Clouthier et al., 2010; Medeiros and Crump, 2012; Trainor and Krumlauf, 2001). Many of these signals are highly conserved among gnathostomes, including Endothelin-1 (EDN1) (Clouthier et al., 2013; Medeiros and Crump, 2012). This peptide is produced in the ectoderm, core mesoderm, and pharyngeal pouch endoderm of the mandibular portion of arch 1 and more caudal arches (Clouthier et al., 1998; Kurihara et al., 1994; Maemura et al., 1996; Yanagisawa et al., 1998) while its cognate receptor, the Endothelin-A receptor (EDNRA), is expressed by all cranial NCCs (Clouthier et al., 1998; Yanagisawa et al., 1998).

Endothelin-1 is produced as a pre-pro molecule, and undergoes two processing steps to yield a mature peptide. The first step is cleavage by Furin proteases to yield a 38 amino acid pro (inactive) form of the molecule, referred to as Big Endothelin-1 (Inoue et al., 1989; Yanagisawa, 1994). While Big Endothelin-1 has some affinity for Endothelin receptors, its activation of receptor signaling is thought to be negligible compared to that of the mature peptide (Inoue et al., 1989; Yanagisawa, 1994; Yanagisawa et al., 1988). Big Endothelin-1 is subsequently processed into the mature 21 amino acid Endothelin-1 molecule by the membrane-bound neutral metalloprotease Endothelin converting enzyme (ECE) (Xu et al., 1994). There are two ECE proteins in mouse, humans and zebrafish (ECE1 and ECE2) (Emoto and Yanagisawa, 1995; Krauss et al., 2014; Xu et al., 1994; Yanagisawa et al., 1998). ECE1 is believed to be the primary converting factor for EDN1 during embryogenesis, as targeted deletion of *Ece1*, but not of *Ece2*, leads to facial defects in mouse embryos resembling those observed in *Edn1* and *Ednra* mutant embryos (Yanagisawa et al., 2000).

Disruption of genes in the EDN1/EDNRA signaling cascade all lead to defects in the ventral craniofacial skeleton (Clouthier et al., 2013). In mice, loss of *Edn1*, *Ednra* or *Ece1* leads to the homeotic transformation of mandibular arch-derived structures into more maxillary-like derivatives. A similar homeotic transformation of the lower jaw is observed in individuals with Auriculocondylar Syndrome, in which EDNRA signaling is disrupted (Gordon et al., 2013; Rieder et al., 2012). Zebrafish possess two *ednra* genes (*ednra1* and *ednra2*), with knockdown of both leading to jaw defects similar to those observed in mouse *Ednra* mutants (Nair et al., 2007). However, a role for ECE1 in craniofacial development is only known in mice, where its loss leads to defects identical to those in *Ednra* mutants (Yanagisawa et al., 2000; Yanagisawa et al., 1998). In this study, we have used several approaches to better understand Ece1 function and regulation during zebrafish facial development. Morpholino-mediated knockdown of *ece1* results in defects similar to those observed in Endothelin pathway mutants, though defects also exist in more dorsal arch derivatives. We also identify Nkx2.5 as a modulator of *Ece1* expression, as *nkx2*.5 morpholino-injected embryos display defects similar to those seen in *ece1* morphants. Importantly, *ece1* mRNA rescues these defects. Similar changes are observed in a subset of *nkx2.5* mutants. These findings reveal that Nkx2.5 is crucial for normal craniofacial development by acting as a novel upstream regulator of Ednra signaling.

RESULTS

Zebrafish *ece1* expression in the heart and pharyngeal arches

Examining protein alignments, zebrafish and mouse Ece1 were highly conserved, with 64% identity for the entire protein, and 75% identity when focusing on the C-terminal peptidase domain (Fig. 1A). In 24 hours post fertilization (hpf) zebrafish embryos, *ece1* was ubiquitously expressed at low levels, though higher expression was evident in the pharyngeal arch ectoderm, heart, brain, and intersegmental vessels (Fig. 1B, E). At 36 hpf, ubiquitous *ece1* expression was still present, with higher levels in the heart and intersegmental vessels (Fig. 1C, F). This pattern was maintained through 48 hpf, with additional *ece1* detected in the heart and pectoral fins and in the dorsal aorta (Fig. 1D, G).

Previous analysis of *Ece1* expression in mouse embryos showed weak expression in the arch mesenchyme and surrounding ectoderm between embryonic days (E) 9.5 - E11.5 (Yanagisawa et al., 1998). However, as EDN1 functions between E8.25 and E9.0 in the mouse (Fukuhara et al., 2004; Ruest and Clouthier, 2009), we began our analysis at E8.5. At this stage, *Ece1* expression was present in the developing heart as well as the mandibular arch (Fig. 1H and Supplemental Fig. 1). At E9.5, *Ece1* expression was faintly observed in the first arch and heart (Fig. 1I). At E10.5, *Ece1* was expressed strongly in the heart and otic vesicle, with weak expression present in the maxillary portion of the first arch (Fig. 1J and Supplemental Fig. 1).

Knockdown of *ece1* leads to craniofacial defects

Loss of mouse *Ece1* disrupts development of mandibular arch-derived structures (Yanagisawa et al., 1998), though the molecular regulation of *Ece1* expression and function during NCC development is unknown. Due to aspects of its early development, the zebrafish model offers an approach to rapidly dissect developmental cues required for NCC patterning, an event that is highly conserved between teleosts and mammals (Clouthier et al., 2010; Schilling and Le Pabic, 2013). We therefore designed and injected a translation blocking Morpholino (MO) against *ece1*. Uninjected control (UIC) and *ece1* ATG MO-embryos were collected at 5 days post fertilization (dpf) and stained with Alcian blue to visualize cartilage. Compared to controls (Fig. 2A–D), both ventral and dorsal arch-derived cartilages were hypoplastic and malformed in *ece1* morphant embryos (Fig. 2F–I); this included Meckel's cartilage fusing to the palatoquadrate (* in Fig. 2H, I), thus disrupting the jaw joint that normally forms between the two cartilages (Kimmel et al., 2001)(phenotype observed in 74% of injected embryos; 70/95). Further, the two halves of Meckel's cartilage were fused at the midline and the anterior tip was deflected ventrally. The ceratohyal was also deflected ventrally and fused to the hyosymplectic and only a single set of ceratobranchials were present (Fig. 2H, I). In addition, the basihyal was extremely hypoplastic (Fig. 2H). In the dorsal jaw, the palatoquadrate was present, though was hypoplastic and missing the pterygoid process (Fig. 2I). The hyosymplectic was dysmorphic, with the hyomandibular region hypoplastic and the symplectic region absent (Fig. 2H, I). Morphants also displayed cardiac edema at 5 dpf, suggestive of a cardiovascular defect (data not shown). These results were confirmed by using a splice blocking MO that blocked splicing of the intron between exons 5 and 6 of the *ece1* gene (Supplemental Fig. 2C, D, I).

While not as efficient, the phenotype in these morphants matched that observed in morphants using the translation blocking (ATG) morpholino (Fig. 2) (phenotype observed in 42% of injected embryos; 44/106). Injection of a scrambled *ece1* MO affected craniofacial development in only 1.7% (2/117) of morphants (Supplemental Fig. 2E, F). Importantly, injection of *ece1* mRNA with the *ece1* splice blocking MO rescued the morphant craniofacial phenotype in 89% (77/87) of embryos at 5 dpf (Supplemental Fig. 2G, H).

These ventral cartilage defects were similar to those observed in *edn1* mutant and morphant embryos (Kimmel et al., 2003; Miller and Kimmel, 2001; Miller et al., 2000). As has been previously reported (Kimmel et al., 2003; Miller and Kimmel, 2001; Miller et al., 2003), in *edn1* MO-injected embryos, hypoplasia of ventral arch derivatives (Meckel's cartilage and the ceratohyal) was observed (Fig. 2K–N) (phenotype observed in >50% of injected embryos). In addition, ceratobranchials 1–4 were absent, leaving only the fifth ceratobranchial containing the pharyngeal teeth (Fig. 2M). Like *ece1* MO-injected embryos, Meckel's cartilage was also fused to the palatoquadrate, disrupting the primary jaw joint. However, unlike *ece1* morphants, dorsal cartilages were relatively normal (Fig. 2N).

Due to the similarities in ventral arch structures between *edn1* morphants/mutants and *ece1* morphants, we examined whether gene expression changes associated with loss of Edn1 function were also observed in *ece1* morphants. *dlx5a* is one the earliest genes induced by Edn1/Ednra signaling (Clouthier and Schilling, 2004; Clouthier et al., 2000) and is expressed throughout the pharyngeal arch mesenchyme early before becoming restricted more dorsally (Fig. 2E and (Clouthier et al., 2000; Talbot et al., 2010). Loss of EDNRA signaling in mouse embryos leads to loss of almost all pharyngeal arch *Dlx5* expression (Ruest et al., 2004). Similarly, compared to expression of *dlx5a* in control larvae, *dlx5* expression in *ece1* morphants was almost completely lost (Fig. 2J), similar to the change observed in *edn1* morphants (Fig. 2O) and *edn1* mutants (Talbot et al., 2010). Thus, Ece1 function in zebrafish appears to act in a similar manner during ventral arch patterning as it does in mammals.

Nkx2-5: a potential regulator of *ece1* expression

While little is known about the regulation of *Ece1* expression in vivo, the human *ECE1* promoter can be bound and activated by NKX2-5 in cultured cardiomyoblasts (Funke-Kaiser et al., 2003). *Nkx2*-5 is expressed in the core arch mesoderm of the mandibular arch in E8.5 mouse embryos (Kasahara et al., 1998; Komuro and Izumo, 1993), with NKX2-5 daughter cells present in the overlying arch ectoderm at E10.5 (Moses et al., 2001). It is therefore possible that NKX2-5 could directly or indirectly regulate *Ece1* expression during pharyngeal arch patterning. We first examined the temporal expression pattern of *Nkx2-5* in the mouse and found that *Nkx2-5* was expressed robustly in the developing heart, pharynx and mandibular arch at E8.5 (Fig. 3A), similar to previous reports (Kasahara et al., 1998; Komuro and Izumo, 1993; Lyons et al., 1995). In the arches, *Nkx2-5* expression was present in the pharyngeal arch ectoderm and endoderm (Fig. 3B), with fainter staining present in the mesenchyme. By E9.5, expression was only observed in the heart (Fig. 3C) and pharynx (Fig. 3D). By E10.5, *Nkx2-5* expression was only present in the heart (Fig. 3E, F).

To further delineate the tissues derived from *Nkx2-5* expressing cells, the fate of *Nkx2-5* daughter cells was determined using *R26R*;*Nkx2-5*$^{cre/+}$ embryos. In E10.5 *R26R*;*Nkx2-5*$^{cre/+}$ embryos, β-galactosidase (β-gal) staining was detected in all pharyngeal arches (Fig. 3G, H). Staining was also observed in the caudal region of the maxillary prominences and in scattered cells throughout the head region (Fig. 3G, H). β-gal activity was confined to the ectoderm, endoderm and mesodermal core (Fig. 3I), with scattered staining was also apparent lining the capillaries within the arch mesenchyme (Fig. 3J), likely representing endothelial cells (Paffett-Lugassy et al., 2013). This correlates with the weak *Nkx2-5* expression observed in the mesenchyme of E8.5 embryos (Fig. 3B). Overall, these findings match well with previous analysis of *Nkx2-5* daughter cell fate in the arches (Paffett-Lugassy et al., 2013).

Zebrafish *nkx2.5* is expressed in the pharyngeal mesoderm

To better characterize *nkx2.5* expression in the zebrafish pharyngeal arches, we examined embryos beginning at 20 somites and observed *nkx2.5* expression in the cardiac precursors condensing at the midline as well as in two lateral domains that correspond to arch mesoderm populations (Fig. 4A, B). This cardiac expression has been well characterized (Alexander et al., 1998; Goldstein and Fishman, 1998; Reiter et al., 1999; Targoff et al., 2013; Targoff et al., 2008). By 24 hpf, *nkx2.5* expression was observed in the mesoderm of arches 3–6 and more weakly in arch 2, while expression in arch 1 was minimal (Fig. 4C, D), a pattern matching that observed in *nkx2.5:GFP* transgenic zebrafish embryos (Choe et al., 2013). In sectioned embryos, *nkx2.5* expression in the arches was primarily observed in the arch mesoderm, surrounded by NCC-derived mesenchyme (Fig. 4E–G). *nkx2.5* was still expressed robustly in the heart at 30 hpf, though mesodermal expression was more diffuse, encompassing arches 1–4 (Fig. 4H, I). This temporal pattern resembles that previously observed for *nkx2.5*+ clusters in developing zebrafish embryos (Paffett-Lugassy et al., 2013). Expression in the dorsal aorta also became evident at this stage (Fig. 4H, I and Supp. Fig. 3A, B). By 36 hpf, *nkx2.5* expression could be seen in the pectoral fin bud (Supp. Fig. 3C, D). This fin bud expression, as well as heart and dorsal aorta expression, persisted through 48 hpf (Supp. Fig. 3E, F). To confirm that *nkx2.5* expression was confined to the arch mesoderm, we performed double fluorescent in situ hybridization (FISH), comparing *nkx2.5* expression with the expression of *hand2*, a ventral mesenchyme marker (Fig. 4J). In 30 hpf embryos, *hand2*-positive NCCs could be seen partially surrounding *nkx2.5*-expressing mesoderm cells in pharyngeal arches 3 and 4, with *nkx2.5* expression considerably weaker in arches 1 and 2 (Fig. 4J).

Loss of zebrafish nkx2.5 leads to defects in pharyngeal arch-derived cartilages

We next examined the function of Nkx2.5 in facial development using MO knockdown. Compared to control embryo skeletons (Fig. 5A–D), 63.8% (n=37/58) of 5 dpf *nkx2.5* morphants stained with Alcian blue exhibited cartilage malformations, of which we identified three classes. In mild morphants (19% of injected larvae (n=11/58)), ventral deflection of Meckel's and the ceratohyal was observed, though facial cartilages were otherwise normally patterned and joint fusions were not observed (data not shown). In moderate morphants (8.6% of larvae analyzed (n=5/58)), there was a mild ventral deflection of Meckel's cartilage and the ceratohyal, with moderate hypoplasia of the otherwise

normally patterned dorsal and ventral arch-derived cartilages and no joint fusions (data not shown). The majority of affected embryos (n=21/58 or 32.6%) fell into the severe class, displaying hypoplasia of all components of the craniofacial skeleton (Fig. 5E–H). This also included changes in Meckel's cartilage, which displayed a ventral downturn and inversion towards the midline (Fig. 5E, H). The majority of embryos examined had normal joint formation (Fig. 5E–H), though the hyosymplectic was hypoplastic and the ventral region truncated, as were all five sets of ceratobranchials (Fig. 5G, H). The palatoquadrate was present but malformed, with an absent pterygoid process (Fig. 5H) and the basihyal was smaller (Fig. 5G) than observed in control embryos (Fig. 5C). Morphants also had varying degrees of cardiac edema that did not correlate with the severity of cartilage defects (data not shown). Co-injection with an p53 MO to limit changes due to MO-induced cell death (Robu et al., 2007) did not alter the phenotype (data not shown).

Since MO-mediated gene knockdown can result in variability in the degree of knockdown and produce off-target affects (Kok et al., 2015), we also assessed craniofacial morphology in a strain carrying a nonsense mutation in the *nkx2.5* gene (generated through TILLING: *nkx2.5*^{vu179}) (Targoff et al., 2013). Both *nkx2.5* mutants and morphants develop ventricular defects, in which ventricular cardiomyocytes transdifferentiate into atrial cardiomyocytes (Targoff et al., 2013; Targoff et al., 2008). However, while cardiac defects were apparent in all *nkx2.5* mutants, the incidence of craniofacial defects in these mutants was 14% (11/77). Most mutants (10/77) displayed a phenotype resembling the mild class of *nkx2.5* morphants, in which Meckel's cartilage was slightly downturned and other viscerocranial elements were slightly hypoplastic (data not shown). However, one mutant displayed a phenotype similar to the severe class of *nkx2.5* morphants, including a downturned Meckel's cartilage containing a slight inversion of the anterior tip and overall hypoplasia of other viscerocranial elements (Fig. 5 I–L), including the basihyal (Fig. 5K). One difference between mutants and morphants was that the pterygoid process of the palatoquadrate was present in *nkx2.5* mutants compared to its absence in *nkx2.5* MO-injected embryos. While there are several reasons that could account for the low penetrance of facial defects in *nkx2.5* mutants (discussed below), the overall phenotypic similarity between the MO and mutant phenotypes suggests that the use of our *nkx2.5* MO is a valid approach. To further study Nkx2.5 function during facial development in an efficient manner, we focused the remainder of our analysis on Nkx-deficient (MO-injected) embryos, as we could generate large numbers of these embryos more easily than would be feasible using *nkx2*.5 mutants, considering the low frequency with which facial defects occurred in mutants.

The ventral defects observed in *nkx2.5* MO-injected embryos are similar to those seen in Endothelin signaling pathway mutants, including *furinA, plcβ3, mef2c, edn1 and ednra1/2* morphants/mutants (Miller et al., 2000; Nair et al., 2007; Talbot et al., 2010; Walker et al., 2007; Walker et al., 2006). Since ventrally-restricted *hand2* expression is disrupted in Endothelin pathway mutants and is suggestive of defects in D-V patterning (Clouthier et al., 2010), we examined a *hand2* reporter transgenic line in which the zebrafish pharyngeal arch-specific enhancer for *hand2* drives expression of *mCherry* (Ikle et al., 2012). In control embryos at 28 hpf, mCherry fluorescence was present in the ventral domain of the pharyngeal arches in a pattern similar to endogenous *hand2* expression (Fig. 5M and data

not shown). Following *nkx2.5* knockdown, mCherry fluorescence was dramatically reduced (Fig. 5N).

Nkx2-5$^{-/-}$ mouse embryos die by E10.0 due to vascular defects (Lyons et al., 1995; Tanaka et al., 1999). However, if the function of NKX2-5 is conserved between mouse and zebrafish, changes in early gene expression should also be conserved. We therefore examined expression of *Hand2* in E9.25 *Nkx2-5*$^{cre/cre}$ embryos, in which the *Nkx2-5* gene is disrupted due to the presence of a Cre expression cassette within the *Nkx2-5* locus (Moses et al., 2001). Though *Hand2* expression comes on shortly before E9.25, weak *Hand2* expression was already observed in the ventral half of the mandibular arch of control embryos (Fig. 5O). In contrast, *Hand2* expression was absent from the pharyngeal arches of *Nkx2-5*$^{cre/cre}$ embryos (Fig. 5P), mirroring the loss we observed in *nkx2.5* morphant zebrafish.

Early pharyngeal arch patterning is disrupted in *nkx2.5* morphants

To better understand the changes in the ventral, intermediate and dorsal pharyngeal arch domains, we examined expression of markers for each of these domains in wild type and *nkx2.5* MO-injected embryos. *dlx5a* and *dlx6a* are key mediators of Ednra signaling (Clouthier et al., 2013). Expression of *dlx5a* in control embryos was observed in arches one and two (Fig. 6A), with expression appearing unchanged in *nkx2.5* morphants (Fig. 6B), in contrast to findings in both mouse and zebrafish Endothelin pathway mutants (Charité et al., 2001; Ruest et al., 2004) (Walker et al., 2007; Walker et al., 2006). In contrast, arch expression of *dlx6a*, also regulated by Ednra signaling (Charité et al., 2001; Ruest et al., 2004; Walker et al., 2007; Walker et al., 2006), was decreased in *nkx2.5* morphants compared to control embryos (Fig. 6C, D). Similar to our findings with mCherry fluorescence (Fig. 5N), *hand2* expression in the pharyngeal arches was almost completely lost in *nkx2.5* morphants (Fig. 6F, H) compared to control embryos (Fig. 6E, G). In contrast, expression of *dlx2a*, which exhibits normal ventral arch expression in zebrafish *edn1* mutants (Miller et al., 2000) but is downregulated in *ednrA1/ednrA2* morphants (Nair et al., 2007), appeared slightly upregulated in *nkx2.5* morphants (Fig. 6J) compared to control embryos (Fig. 6I). In addition, expression of *dlx3b*, an intermediate arch domain marker (Fig. 6K) whose expression is downregulated in Endothelin mutants (Clouthier et al., 2010; Talbot et al., 2010), was also absent in *nkx2.5* morphants (Fig. 6L).

The discordance in *dlx5a* gene expression compared to the other observed changes was surprising, though this could reflect the level of gene expression change, as small changes in gene expression can be difficult to detect by ISH (Vieux-Rochas et al., 2010). We therefore performed quantitative RT-PCR using total RNA from 24 hpf control and *nkx2.5* morphant embryos. This analysis revealed that expression of both *dlx5a* and *dlx6a* were significantly downregulated, with *dlx6a* expression (0.51) lower than that of *dlx5a* (0.76), matching the ISH results (Fig. 6Q). Expression of *hand2* (0.72) and *dlx3b* (0.54) were also downregulated, with remaining expression likely due to gene expression at other sites in the embryo (Fig. 6Q). While expression of *dlx2a* appeared increased by ISH, the increase was not statistically significant as determined by qRT-PCR. Thus, knockdown of *nkx2.5* expression leads to gene expression changes that resemble those of other Endothelin pathway mutant/morphants.

Loss of Nkx2.5 impacts expression of Endothelin pathway family members

The ventral defects and early gene expression changes observed in *nkx2.5* morphants are similar to those seen in *ece1* morphants, suggesting a potential relationship between Nkx2.5 and Ece1. Because the human *ECE1* promoter can be bound and activated by NKX2-5 in cardiomyoblasts (Funke-Kaiser et al., 2003), we examined whether Ece1 was a potential Nkx2.5 target within the Ednra signaling pathway. By ISH, *ece1* expression was decreased in the pharyngeal arches of *nkx2.5* morphants at 24 hpf (Fig. 6N) compared to the expression of *ece1* expression in control embryos (Fig. 6M). By qRT-PCR, expression was unchanged in *nkx2.5* morphant embryos (Fig. 6Q), potentially indicating that expression was unaffected in other areas of the embryo in which *ece1* is expressed (Yanagisawa et al., 2000; Yanagisawa et al., 1998). To determine if loss of Nkx2.5 also affected *edn1* transcription, we examined *edn1* expression in control and *nkx2.5* morphant larvae at 24 hpf (Fig. 6O, P). *edn1* expression was detected in the pharyngeal arch ectoderm in both wild type (Fig. 6O) and *nkx2.5* MO-injected (Fig. 6P) larvae, though expression in *nkx2.5* morphants appeared slightly lower. By qRT-PCR, expression was downregulated ~50% in *nkx2.5* morphants (Fig. 6Q). While these experiments cannot determine whether the function of Nkx2.5 on *ece1* is direct or indirect, it does appear that loss of Nkx2.5 disrupts the Endothelin signaling network at several points.

During ventricular development, Nkx2.5 and Nkx2.7 function together to maintain ventricular identity (Targoff et al., 2013; Targoff et al., 2008). We thus examined whether downregulation of Nkx2.5 in *nkx2.5* morphants affected *nkx2*.7 expression. By qRT-PCR, the expression of *nkx2*.7 was downregulated ~25% (Fig 6Q). While it is unknown whether Nkx2.5 can induce *nkx2*.7 expression in vivo, our results suggest that the Nkx2.5 phenotype may represent a broader change in Nkx gene expression.

Craniofacial defects in *nkx2.5* MO-injected embryos are rescued with *ece1* mRNA

To determine whether Nkx2.5 was required for *ece1* expression, we attempted to rescue the *nkx2.5* morphant phenotype by over-expressing *ece1*. Capped *ece1* mRNA was injected at the one-cell stage, followed by injection of the *nkx2.5* MO, with larvae analyzed at 5 dpf for cartilage development. *nkx2.5* morphants had defects in viscerocranial and neurocranial elements and occasional joint fusions (Fig. 5E–H; Fig. 7E–G), while overexpression of *ece1* mRNA alone did not result in obvious changes in arch-derived elements (Fig. 7I–K). However, co-injection of *ece1* mRNA led to a dramatic rescue in development of arch-derived elements in *nkx2.5* morphants (Fig. 7M–O). As described above, quantification of *nkx2.5* morphants showed that 63.8% (n=37/58) exhibited cartilage malformations with the *nkx2.5* MO alone (Fig. 7Q). When coinjected with *ece1* mRNA, the number of malformed embryos dropped to 31.1% (n=23/74), representing a 51% rescue over MO injection alone. Further, embryos exhibiting severe defects showed the highest degree of rescue, with the incidence of defects going from 36.2% (n=21/58) when embryos were injected with MO alone to 12.2% (n=9/74) when co-injected with MO and *ece1* mRNA (Fig. 7Q). This represents a 66.3% rescue of severe defects. The incidence of moderate and mild defects also decreased in *nkx2.5* morphants receiving *ece1* mRNA, though it was not possible to determine whether embryos that still had moderate or mild defects actually represented formally severe mutants with improved cartilage development.

One explanation of improved ventral cartilage development in *nkx2.5* morphants also receiving *ece1* mRNA is that early gene expression associated with pharyngeal arch patterning was rescued. We thus examined the change in *hand2* expression within the ventral arch of MO and MO/mRNA embryos. Injection of the *nkx2.5* MO led to a significant downregulation of *hand2* expression in the pharyngeal arches (Fig. 7H). *hand2* expression following injection of *ece1* mRNA appeared similar to that observed in control embryos (Fig. 7L). In contrast, *nkx2.5* morphants also receiving *ece1* mRNA displayed increased *hand2* expression (Fig. 7P) compared to MO injection alone (Fig. 7H), although it did not appear to reach the level observed in control embryos (Fig. 7D). Thus, the observed rescue of ventral arch defects in *nkx2.5* MO-injected embryos by *ece1* mRNA does involve partial restoration of the Endothelin signaling network.

DISCUSSION

Edn1/Ednra signaling is one of the key events during D-V patterning of NCCs in the pharyngeal arches in gnathostomes (jawed vertebrates) (Clouthier et al., 2013). Loss of this signaling leads to defects in ventral and intermediate arch derivatives. The key regulatory step is the processing of big EDN1 into mature EDN1 by ECE1 (Xu et al., 1994). We have shown here that Nkx2.5 is a key regulator of *ece1* expression in both mouse and zebrafish and thus has a critical role in facial morphogenesis not previously recognized.

Penetrance of the craniofacial defects in *nkx2.5* mutants

While *nkx2*.5 morphant and mutant embryos have similar craniofacial defects, the penetrance of such defects in *nkx2*.5 mutants is low. This may relate to the sensitivity of Ednra signaling to modifier effects. Mutations in the gene encoding PLCB4, part of the intracellular signaling pathway induced by EDNRA signaling, result in Auriculocondylar Syndrome (ACS) in humans, though the severity of the phenotype can vary among family members carrying the same mutation (Rieder et al., 2012). Likewise, mutations in *NKX2-5* are associated with congenital heart disease (CHD) (Reamon-Buettner and Borlak, 2010), though identical mutations within *NKX2*-5 can result in different CHDs in different individuals (Abou Hassan et al., 2015; Reamon-Buettner and Borlak, 2010). These findings illustrate that EDNRA signaling may be particularly sensitive to the action of genetic modifiers.

Another possibility is that the morphant phenotype reflects off-target effects of the morpholino. Recently, Kok et al. showed that morphant phenotypes in 80 different genes were not recapitulated in 80% of corresponding mutant fish (Kok et al., 2015). However, there are several plausible explanations that could explain this discordance besides off-target effects (Blum et al., 2015). Mutations generated by TILLING or genome editing may represent hypomorphic alleles due to incomplete loss of function or continued expression of a portion of the mutant gene due to cryptic start sites or altered splicing (Stainier et al., 2015). In these instances, a morpholino knockdown of the same gene could result in a more complete loss of gene function. In addition, at least some genetic pathways can compensate for complete gene loss, but not for gene knockdown, by upregulating other genes (Rossi et al., 2015). Such compensation during facial development is observed between *Msx1* and

Msx2 (Han et al., 2007). In this case, a strong loss of function allele would result in the activation of a compensatory mechanism whereas low level gene expression in morphants would be above the threshold for induction of compensation. More detailed interrogation of potential compensation for loss of Nkx2.*5* function is required to address these questions.

ECE1/NKX2-5 functions in mouse and zebrafish facial morphogenesis

In *Nkx2-5*$^{cre/+}$ embryos, *Nkx2-5* daughter cells were present in the pharyngeal arch ectoderm (Moses et al., 2001) and core mesoderm and vasculature (Paffett-Lugassy et al., 2013) at E10.5. We have shown here that these Nkx2-5 lineage cells first express *Nkx2-5* around E8.5 for less than 24 hours, corresponding to the time during which EDNRA signaling establishes D-V polarity within the pharyngeal arches (Fukuhara et al., 2004; Ruest and Clouthier, 2009). After E9.5, EDNRA signaling is no longer required (Ruest et al., 2005), likely due in part to the function of BMPs (Alexander et al., 2011). This matches well with our expression data showing that mouse *Nkx2-5* expression is normally downregulated after E9.5. However, while ventral arch defects are similar to those observed in other Endothelin-pathway mutants, *ece1* morphants and *nkx2.5* morphants and mutants also had defects in dorsal arch cartilages. Interestingly, in *Ednra*$^{-/-}$ mouse embryos, bones that compose the zygomatic arch (including the jugal) are hypoplastic (Ruest et al., 2004), suggesting that EDNRA signaling also contributes to the development of more posterior maxillary derivatives that derive from the dorsal mandibular arch. It is worth noting that the zebrafish *edn1* mutation (Miller et al., 2000) is likely not a complete loss-of-function allele (Jamie Nichols, personal communication), meaning that the *edn1* mutant phenotype may actually only produce a hypomorphic craniofacial phenotype. Answering these questions will require in depth structural analysis and earlier gene expression profiling.

Another explanation for the defects in dorsal derivatives is that Nkx2.5-induced Ece1 activity (either direct or indirect) is required for the processing of other proteins beside Edn1. While one candidate is Edn3, a molecule required for iridophore development in zebrafish larva (Krauss et al., 2014), EDN3 does not play a role in murine facial development (Baynash et al., 1994) and has a weak binding affinity for Ednra (Breu et al., 1995; Lee et al., 1994). Besides EDNs, metalloproteases like ECE1 (including neutral endopeptidase (NEP) and angiotensin-converting enzyme (ACE)) often have broad specificity; indeed, ECE1 can hydrolyze a number of peptides, including bradykinin, neurotensin, substance P and atrial natriuretic peptide (ANP) (Johnson et al., 1999; Nakayama et al., 2012). Based on phylogeny, Ece1 has a more ancient origin than does Edn1, further suggesting functional roles outside of big Edn1 cleavage (Hyndman and Evans, 2007). While these findings suggest that ECE proteins can act on other proteins, further experiments are required to determine whether the function of such proteins can explain the dorsal defects observed in *nkx2.5* morphants and mutants.

Like our results shown here, knockdown of *grainyhead-like 3* (*grhl3*) in zebrafish embryos also results in defects in both dorsal and ventral cartilage derivatives of the first arch (Dworkin et al., 2014). *grhl3* morphants have elevated cell death and decreased proliferation within the arches, accounting for the hypoplasia. Grhl3 appears to induce *edn1* expression, leading to the hypothesis that loss of Endothelin signaling is the underlying cause of the

grhl3 morphant phenotype. This is supported by the finding in zebrafish that Edn1 promotes both early patterning and proliferation of the NCC-derived mesenchyme in the mandibular arch (Sasaki et al., 2013) and raise the possibility that Endothelin signaling is involved in the development of a greater array of facial elements than previously thought. In addition, this may strengthen the idea that Nkx2.5 regulates both *ece1* and *edn1* expression. We showed that *ece1* levels changed by ISH but not by qRT-PCR, while *edn1* levels changed in both assays. As previously mentioned, *Ece1* expression in mice is quite broad, so a failure to see downregulation by qRT-PCR may be due to continued expression elsewhere in the larvae. In addition, it is unclear how absence of Edn1 alone could be rescued by additional Ece1, considering that the level of Ece1 is normally sufficient for craniofacial development. While NKX2-5 can regulate rat *Ece1* expression (Funke-Kaiser et al., 2003), human *EDN1* expression appears to be negatively regulated by NKX2-3 (Yu et al., 2011). As our qRT-PCR for *edn1* and *ece1* in *nkx2.5* morphants illustrate, understanding Nkx2.5 function during facial morphogenesis will require dissecting its individual roles in regulating the expression of Endothelin pathway members.

Gene expression changes in *nkx2.5* morphants

Members of the Dlx family of transcription factors are also crucial mediators of Ednra signaling. The loss of *dlx3b* but not *dlx2a* in *nkx2.5* morphants is similar to what has been observed in *edn1* mutants (Walker et al., 2006), though the reduction in *dlx5a* and *dlx6a* expression, while present, was more modest compared to *edn1* mutants. However, DLX5/DLX6 directly activates *Hand2* expression (Charité et al., 2001). As *hand2* expression decreased in both *nkx2.5* MO-injected embryos and *Nkx2-5* mutant mouse embryos, this modest reduction in *dlx5a/6a* expression in the morphants is functionally sufficient to impact downstream effectors. While it is possible that Nkx2.5 directly activates the *hand2* arch enhancer (through putative Nkx2.5 binding sites in the enhancer (Ikle et al., 2012)), *hand2* expression in the lateral plate mesoderm is unaffected in *nxk2.5* mutants (Targoff et al., 2013), arguing against this possibility. Further, both *Hand2* and *Dlx3* are transcriptionally downstream of DLX5/DLX6 (Barron et al., 2011; Depew et al., 2002). As *dlx3b* expression is lost in *nkx2.5* MO-injected embryos, Nkx2.5 must be acting in part upstream of Hand2. That Dlx gene expression is not lower could suggest that other signaling pathways can partially compensate for loss of Edn1 activity following knockdown of *nkx2*.5, one candidate being Bmp signaling (Alexander et al., 2011). In addition, we cannot rule out that Ece2a/b can compensate for loss of Ece1, though such compensation in mice is not observed (Yanagisawa et al., 2000). Thus, decreased Nkx2.5 levels are sufficient to disrupt the Endothelin signaling pathway.

Coordination of Nkx family members in transcriptional regulation

The zebrafish genome contains two additional NKX2-5 paralogs: Nkx2.3 and Nkx2.7. In vertebrates, NKX molecules often act cooperatively or redundantly to regulate developmental processes. Pharynx development is disrupted in mice lacking both *Nkx2-5* and *Nkx2-6* (Tanaka et al., 2001), though loss of either individually has no effect on the pharynx (Tanaka et al., 1999; Tanaka et al., 2000). Similar relationships are also seen in Nkx function during zebrafish cardiac development. As previously mentioned, loss of *nkx2.5* results in loss of ventricular cardiomyocytes and concomitant increase in atrial

cardiomyocytes (Targoff et al., 2008). While loss of *nkx2.7* results in very mild ventricular defects, loss of *nkx2.7* in a *nkx2.5* mutant background greatly exacerbates the ventricular phenotype, illustrating that Nkx proteins function cooperatively to maintain ventricular identity of cardiomyocytes (Targoff et al., 2013). Though relationship of Nkx2.5 and Nkx2.7 to each other's expression profiles is not known for ventricular development, we showed that global *nkx2*.7 expression is downregulated in *nkx2.5* morphants, indicating that the relationship of these two Nkx genes may be complex and involve transcription and post-transcriptional components. It will therefore be important to determine whether facial morphogenesis is disrupted in *nkx2.5/nkx2.7* double mutants, whether this is reflected in more severe changes in early arch gene expression and whether this accounts for the low penetrance of facial defects in *nkx2*.5 mutants alone. It is worth noting that jaw abnormalities have been reported in *nkx2.5/2.7* double morphants (Targoff et al., 2008). It is also possible that Nkx2.3 can function cooperatively or redundantly with Nkx2.5 during cranial NCC patterning, though *nkx2.3* expression occurs in the pharyngeal endoderm and ectoderm (Biben et al., 2002; Pabst et al., 1997). Since *nkx2.5* expression occurs in the mesoderm (this study and (Choe et al., 2013)), a redundant or shared contribution towards NCC development is harder to envision. Analysis of facial development in *nkx2.3* mutants will be required to better understand this possibility.

Recent discoveries have linked changes in EDNRA signaling to human birth defect syndromes, including Auriculocondylar Syndrome (ACS) (Gordon et al., 2015) and Mandibulofacial Dysostosis with Alopecia (Gordon et al., 2015). However, many other human birth defect syndromes exist with similar craniofacial phenotypes but without defined genetic changes. Our study provides novel evidence that *NKX2*-5 should be considered a new EDNRA pathway component and potential target in gene-phenotype investigations when investigating craniofacial dysmorphologies.

MATERIALS AND METHODS

Animal Use

All animal use was approved by Institutional Animal Care and Use Committees at the University of Indiana, University of California, San Diego, Columbia University and the University of Colorado Anschutz Medical Campus and in accordance with "Guide for Care and Use of Laboratory Animals", as defined by NIH.

Fish strains and genotyping—Fish were raised and maintained under standard conditions (Westerfield, 1993). Zebrafish embryos for morpholino injection were collected from natural matings of TAB wild type fish; embryos were cultured and staged as described (Kimmel et al., 1995). Generation and genotyping of the *nkx2.5*^{vu179} allele has been previously described (Targoff et al., 2013). The mutation is recessive lethal and acts as a loss-of-function allele. The strain is available upon request.

Mouse strains and genotyping—Creation and genotyping of the B6.129S4-*Gt(ROSA)26Sor*^{tm1Sor}/J (*R26R*) strain (Jackson Laboratories Stock #003474) has been previously described (Soriano, 1999), as has the creation of B6129S1-*Nkx2-5*$^{tm1(cre)Rjs}$/J (*Nkx2-5*^{cre}) mutant mice (Moses et al., 2001)(Jackson Laboratories Stock #030047). For the

latter, a *Cre* expression cassette was inserted in frame in place of exon 2 of *Nkx2-5*, in essence creating a null allele of *Nkx2-5* (Moses et al., 2001). *Nkx2-5*$^{cre/cre}$ embryos die around E10.0 from cardiovascular defects similar to those observed in *Nkx2-5*$^{-/-}$ embryos (Lyons et al., 1995). Genotyping was performed using a general Cre identification protocol (Tavares et al., 2012). For embryonic staging, E0.5 was defined as the morning that the vaginal plug was observed.

Morpholino oligonucleotide injection

Morpholinos were diluted to 2.5 ng/nl and injected into embryos at the 1–4 cell stage using an Olympus SZX16 stereomicroscope and a Harvard Apparatus Pico Injector PLI-100. Either 2.5% fluorescein dextran (10,000 MW, lysine fixable, Invitrogen) or 0.1% phenol red was used to track injections. An *edn1* translation blocking morpholino was synthesized by Gene Tools (Eugene, OR) using a previously published sequence (Miller and Kimmel, 2001). This morpholino elicits joint fusions and loss of cartilage consistent with loss of Endothelin-1. A *nkx2.5* translation blocking morpholino was synthesized by Gene Tools using a previously published sequence (Targoff et al., 2008; Tu et al., 2009). To knockdown Ece1 function, a translation blocking morpholino was designed to the translation start sequence of *ece1* (5'-AAGTAGACATCTGAGGGAAATGTAC-3'). An *ece1* splice blocking morpholino was designed to inhibit splicing of exon 5 and exon 6 (5'-TGTGTGTATCTGAGGTCACCTGATT-3'). A dose-response curve identified 5 ng of morpholino as a moderate dose that routinely resulted in craniofacial phenotypes with only minimal lethality. To control for specificity of the *ece1* morpholinos, we also designed and injected an *ece1* scrambled morpholino (5'-AACTACACATCTCAGGCAAATCTAC-3'). All morpholinos were synthesized by Gene Tools. To suppress potential morpholino-induced cell death, morpholino injections also included 2 ng of a p53 morpholino (Robu et al., 2007).

Efficacy of the *ece1* splice blocking morpholino was confirmed by reverse transcription (RT)-PCR using the following primers: 5'-TCAGCAACCTGTGGGAACAT-3' (in exon 4) and 5'-CTCCTGGAAGTTATCCTTCTC-3' (in exon 6). As the design of the *ece1* morpholino should result in exon skipping (Draper et al., 2001), RT-PCR using these primers should result in a 224 bp band when splicing occurs properly and a 99 bp band when splicing is disrupted (thus excluding exon 5).

mRNA synthesis and injection

ece1 mRNA was synthesized from the pExpress-*ece1* plasmid (Open Biosystems) using the SP6 mMESSAGE mMACHINE In Vitro Transcription Kit (Ambion). *ece1* mRNA was diluted in nuclease-free water and mixed with 2.5% fluorescein dextran for a final concentration of 200 ng/ul. 1 nl of solution was injected into zebrafish embryos at the single cell stage as described above.

Bone and cartilage staining

Zebrafish larvae were anesthetized in Tricaine, then fixed for 1 hour in 4% paraformaldehyde (PFA). Alcian blue and alizarin red staining was performed as previously described (Walker and Kimmel, 2007).

Whole mount in situ hybridization (ISH)

For ISH analysis in zebrafish, at least 20 embryos were examined per probe. Embryos were collected from wild-type matings and fixed in 4% paraformaldehyde. Embryos to be used for later stages were placed in phenylthiourea (PTU) at 24 hpf to prevent pigment formation. Antisense RNA probes were synthesized from cDNAs and labeled with digoxigenin using the DIG RNA Labeling kit (Roche). The *nkx2.5* ISH probe was created by cutting a *nkx2.5* cDNA (cloned into pME18S-FL3; Open Biosystems) with *Eco*RI and *Not*I and then subcloning into pBluescriptSK+ cut with *Eco*RI and *Not*I. The resulting plasmid was linearized with *Eco*RI and labeled antisense RNA probe synthesized using T3 RNA polymerase and the DIG RNA Labeling kit (Roche). *ece1* probe was created from an *ece1* cDNA (in pExpress-1; Open Biosystems) linearized with *Bam*HI and labeled using T7 RNA polymerase. Published probes included *dlx2a, dlx3b*, *dlx5a* and *dlx6a* (Talbot et al., 2010) (gifts from C. Kimmel), *hand2* and *edn1* (Alexander et al., 2011) (gifts from T. Schilling). Whole mount ISH was adapted from previously described protocols (Ikle et al., 2012). Embryos were mounted in 100% glycerol, coverslipped, and photographed under brightfield using an Olympus BX51 compound microscope fitted with a DP71 digital camera. For sectional analysis, stained zebrafish embryos were embedded in agar as described (Westerfield, 1993). 30 micron sections were cut and photographed under Nomarski optics on an Olympus BX51 microscope.

For fluorescent ISH, probes were labeled and developed as described (Talbot et al., 2010). Embryos were mounted in 100% glycerol and imaged using an Olympus BX51 compound microscope and a DP-71 digital camera.

Whole mount ISH analysis in mouse embryos (n=3) was performed as previously described (Clouthier et al., 1998).

Sectional in situ hybridization

Embryos were fixed overnight in 4% PFA at 4°C, then transferred to a 30% sucrose solution until the embryo sank. Following a 1:1 Sucrose:OCT wash for 1 hour, embryos were embedded in OCT, with 12 micron sections cut using a Leica 3700 cryostat. ISH was then performed as previously described (Hendershot et al., 2007). Analysis and photography of stained sections was performed as described above.

Real time PCR

Control and *nkx2.5* morphant embryos were collected at 24 hpf into TRI reagent (Zymo Research), homogenized and stored at −80°C. For RNA collection, 40–50 larvae were pooled; this was performed for three separate morpholino injections. RNA was collected using the Direct-zol RNA MiniPrep kit (Zymo Research). Samples were DNase I-treated to eliminate gDNA contamination. cDNA was prepared from total RNA using the Quantitect cDNA Synthesis Kit (Qiagen). Real Time quantitative PCR was performed using the reagents and protocols from the Quantitect SYBR Green PCR Kit (Qiagen). Quantitect Assay primers (predesigned primers from Qiagen against *hand2*, *dlx2a*, *dlx3b*, *dlx5a*, *dlx6a*, *edn1*, *nkx2*.5 and *nkx2*.7) were resuspended to a 10× stock as recommended by the manufacturer; primers were used at a 1× concentration. To amplify *ece1*, the following

primers were used: 5'-CCTACTACAACCCGACAAAGAA-3' and 5'-CACACCTATCCCACCGAAAT-3'. For each RT-PCR reaction, 5 ng of cDNA was used. RT-PCR and subsequent data analysis was performed using a CFX Connect Real-Time System (BioRad). Statistical analysis of resulting data by unpaired two-tailed t-test was performed using Prism software (GraphPad).

Statistical and bioinformatics analysis

Statistics were performed using a two-tailed Fisher's exact test (GraphPad). Protein alignment was done using The Sequence Manipulation Suite (http://www.bioinformatics.org/sms2/pairwise_align_protein.html).

β-galactosidase (β-gal) staining

Embryos for whole mount β-gal staining were processed, stained, sectioned and examined as previously described (Ruest et al., 2003).

Supplementary Material

Refer to Web version on PubMed Central for supplementary material.

Acknowledgments

The authors would like to thank Holly Buttermore, Crystal Woods and Alicia Navetta for technical assistance, Kristin Artinger for assistance in photographing zebrafish larvae and advice during the experiments and Noriaki Emoto for helpful discussions. This work was supported by grants AR061392 from NIH/NIAMS (to A.B.F.), HD043489 from NIH/NICHD and HL099002 from NIH/NHBLI (to K.L.T), HL108599 from NIH/NHLBI (to D.Y.), a NIH/NHLBI training award added to T32 GM008497 (to J.M.I) and DE018899 and DE023050 from NIH/NIDCR (to D.E.C.).

References

Abou Hassan OK, Fahed AC, Batrawi M, Arabi M, Refaat MM, DePalma SR, Seidman JG, Seidman CE, Bitar FF, Nemer GM. *NKX2-5* mutations in an inbred consanguineous population: genetic and phenotypic diversity. Sci. Rep. 2015; 5:8848. [PubMed: 25742962]

Alexander C, Zuniga E, Blitz IL, Wada N, LePabic P, Javidan Y, Zhang T, Cho KW, Crump JG, Schilling TF. Combinatorial roles for Bmps and Endothelin 1 in patterning the dorsal-ventral axis of the craniofacial skeleton. Development. 2011; 138:5135–5146. [PubMed: 22031543]

Alexander J, Stainier DY, Yelon D. Screening mosaic F1 females for mutations affecting zebrafish heart induction and patterning. Dev. Genet. 1998; 22:288–299. [PubMed: 9621435]

Barron F, Woods C, Kuhn K, Bishop J, Howard MJ, Clouthier DE. Downregulation of *Dlx5* and *Dlx6* expression by Hand2 is essential for initiation of tongue morphogenesis. Development. 2011; 138:2249–2259. [PubMed: 21558373]

Baynash AG, Hosoda K, Giaid A, Richardson JA, Emoto N, Hammer RE, Yanagisawa M. Interaction of endothelin-3 with endothelin-B receptor is essential for development of epidermal melanocytes and enteric neurons. Cell. 1994; 79:1277–1285. [PubMed: 8001160]

Biben C, Wang CC, Harvey RP. *NK-2* class homeobox genes and pharyngeal/oral patterning: *Nkx2-3* is required for salivary gland and tooth morphogenesis. Int. J. Dev. Biol. 2002; 46:415–422. [PubMed: 12141427]

Blum M, De Robertis EM, Wallingford JB, Niehrs C. Morpholinos: Antisense and Sensibility. Dev. Cell. 2015; 35:145–149. [PubMed: 26506304]

Breu V, Hashido K, Broger C, Miyamoto C, Furuichi Y, Hayes A, Kalina B, Loffler BM, Ramuz H, Clozel M. Separable binding sites for the natural agonist endothelin-1 and the non-peptide

antagonist bosentan on human endothelin-A receptors. Eur. J. Biochem. 1995; 231:266–270. [PubMed: 7628480]

Charité J, McFadden DG, Merlo GR, Levi G, Clouthier DE, Yanagisawa M, Richardson JA, Olson EN. Role of Dlx6 in regulation of an endothelin-1-dependent, *dHAND* branchial arch enhancer. Genes Dev. 2001; 15:3039–3049. [PubMed: 11711438]

Choe CP, Collazo A, Trinh le A, Pan L, Moens CB, Crump JG. Wnt-dependent epithelial transitions drive pharyngeal pouch formation. Dev Cell. 2013; 24:296–309. [PubMed: 23375584]

Clouthier DE, Garcia E, Schilling TF. Regulation of facial morphogenesis by endothelin signaling: insights from mouse and fish. Am. J. Med. Genet., Part A. 2010; 152A:2962–2973. [PubMed: 20684004]

Clouthier DE, Hosoda K, Richardson JA, Williams SC, Yanagisawa H, Kuwaki T, Kumada M, Hammer RE, Yanagisawa M. Cranial and cardiac neural crest defects in endothelin-A receptor-deficient mice. Development. 1998; 125:813–824. [PubMed: 9449664]

Clouthier DE, Passos-Bueno MR, Tavares ALP, Lyonnet S, Amiel J, Gordon CT. Understanding the basis of Auriculocondylar syndrome: Insights from human, mouse and zebrafish studies. Am. J. Med. Genet, Part C. 2013; 163:306–317.

Clouthier DE, Schilling TF. Understanding endothelin-1 function during craniofacial development in the mouse and zebrafish. Birth Defects Res. (Part C). 2004; 72:190–199.

Clouthier DE, Williams SC, Yanagisawa H, Wieduwilt M, Richardson JA, Yanagisawa M. Signaling pathways crucial for craniofacial development revealed by endothelin-A receptor-deficient mice. Dev. Biol. 2000; 217:10–24. [PubMed: 10625532]

Depew MJ, Lufkin T, Rubenstein JL. Specification of jaw subdivisions by *Dlx* genes. Science. 2002; 298:381–385. [PubMed: 12193642]

Draper BW, Morcos PA, Kimmel CB. Inhibition of zebrafish *fgf8* pre-mRNA splicing with morpholino oligos: a quantifiable method for gene knockdown. genesis. 2001; 30:154–156. [PubMed: 11477696]

Dworkin S, Simkin J, Darido C, Partridge DD, Georgy SR, Caddy J, Wilanowski T, Lieschke GJ, Doggett K, Heath JK, et al. *Grainyhead-like 3* regulation of *endothelin-1* in the pharyngeal endoderm is critical for growth and development of the craniofacial skeleton. Mech. Dev. 2014; 133:77–90. [PubMed: 24915580]

Emoto N, Yanagisawa M. Endothelin converting enzyme-2: a membrane-bound, phosphoramidon-sensitive metalloprotease with acidic pH optimum. J. Biol. Chem. 1995; 70:15262–15268.

Fukuhara S, Kurihara Y, Arima Y, Yamada N, Kurihara H. Temporal requirement of signaling cascade involving endothelin-1/endothelin receptor type A in branchial arch development. Mech. Dev. 2004; 121:1223–1233. [PubMed: 15327783]

Funke-Kaiser H, Lemmer J, Langsdorff CV, Thomas A, Kovacevic SD, Strasdat M, Behrouzi T, Zollmann FS, Paul M, Orzechowski HD. Endothelin-converting enzyme-1 (ECE-1) is a downstream target of the homeobox transcription factor Nkx2-5. FASEB J. 2003; 17:1487–1489. [PubMed: 12824294]

Goldstein AM, Fishman MC. Notochord regulates cardiac lineage in zebrafish embryos. Dev. Biol. 1998; 201:247–252. [PubMed: 9740662]

Gordon CT, Petit F, Kroisel PM, Jakobsen L, Zechi-Ceide RM, Oufadem M, Bole-Feysot C, Pruvost S, Masson C, Tores F, et al. Mutations in endothelin 1 cause recessive auriculocondylar syndrome and dominant isolated question-mark ears. Am. J. Hum. Genet. 2013; 93:1118–1125. [PubMed: 24268655]

Gordon CT, Weaver KN, Zechi-Ceide RM, Madsen EC, Tavares AL, Oufadem M, Kurihara Y, Adameyko I, Picard A, Breton S, et al. Mutations in the endothelin receptor type A cause mandibulofacial dysostosis with alopecia. Am. J. Hum. Genet. 2015; 96:519–531. [PubMed: 25772936]

Han J, Ishii M, Bringas P Jr, Maas RL, Maxson RE Jr, Chai Y. Concerted action of Msx1 and Msx2 in regulating cranial neural crest cell differentiation during frontal bone development. Mech. Dev. 2007; 124:729–745. [PubMed: 17693062]

Hyndman KA, Evans DH. Endothelin and endothelin converting enzyme-1 in the fish gill: evolutionary and physiological perspectives. J. Exp. Biol. 2007; 210:4286–4297. [PubMed: 18055618]

Ikle JM, Artinger KB, Clouthier DE. Identification and characterization of the zebrafish pharyngeal arch-specific enhancer for the basic helix-loop-helix transciption factor Hand2. Dev. Biol. 2012; 368:118–126. [PubMed: 22595513]

Inoue A, Yanagisawa M, Takuwa Y, Mitsui Y, Kobayashi M, Masaki T. The human preproendothelin-1 gene. J. Biol. Chem. 1989; 264:14954–14959. [PubMed: 2670930]

Johnson GD, Stevenson T, Ahn K. Hydrolysis of peptide hormones by endothelin-converting enzyme-1. A comparison with neprilysin. J. Biol. Chem. 1999; 274:4053–4058. [PubMed: 9933597]

Kasahara H, Bartunkova S, Schinke M, Tanaka M, Izumo S. Cardiac and extracardiac expression of Csx/Nkx2.5 homeodomain protein. Circ. Res. 1998; 82:936–946. [PubMed: 9598591]

Kimmel CB, Ballard WW, Kimmel CB, Ullmann B, Schilling TF. Stages of embryonic development of the zebrafish. Dev. Dyn. 1995; 203:253–310. [PubMed: 8589427]

Kimmel CB, Miller CT, Moens CB. Specification and morphogenesis of the zebrafish larval head skeleton. Dev. Biol. 2001; 233:239–257. [PubMed: 11336493]

Kimmel CB, Ullmann B, Walker M, Miller CT, Crump JG. Endothelin 1-mediated regulation of pharyngeal bone development in zebrafish. Development. 2003; 130:1339–1351. [PubMed: 12588850]

Kok FO, Shin M, Ni CW, Gupta A, Grosse AS, van Impel A, Kirchmaier BC, Peterson-Maduro J, Kourkoulis G, Male I, et al. Reverse genetic screening reveals poor correlation between morpholino-induced and mutant phenotypes in zebrafish. Dev. Cell. 2015; 32:97–108. [PubMed: 25533206]

Komuro I, Izumo S. *Csx* : a murine homeobox-containing gene specifically expressed in the developing heart. Proc. Natl. Acad. Sci. U.S.A. 1993; 90:8145–8149. [PubMed: 7690144]

Krauss J, Frohnhofer HG, Walderich B, Maischein HM, Weiler C, Irion U, Nusslein-Volhard C. Endothelin signalling in iridophore development and stripe pattern formation of zebrafish. Biol. Open. 2014; 3:503–509. [PubMed: 24857848]

Kurihara Y, Kurihara H, Suzuki H, Kodama T, Maemura K, Nagai R, Oda H, Kuwaki T, Cao W-H, Kamada N, et al. Elevated blood pressure and craniofacial abnormalities in mice deficient in endothelin-1. Nature. 1994; 368:703–710. [PubMed: 8152482]

Lee JA, Elliott JD, Sutiphong JA, Friesen WJ, Ohlstein EH, Stadel JM, Gleason JG, Peishoff CE. Tyr-129 is important to the peptide ligand affinity and selectivity of human endothelin type A receptor. Proc. Natl. Acad. Sci. U.S.A. 1994; 91:7164–7168. [PubMed: 8041764]

Lyons I, Parsons LM, Hartley L, Li R, Andrews JE, Robb L, Harvey RP. Myogenic and morphogenetic defects in the heart tubes of murine embryos lacking the homeo box gene *Nkx2-5*. Genes Dev. 1995; 9

Maemura K, Kurihara H, Kurihara Y, Oda H, Ishikawa T, Copeland NG, Gilbert DJ, Jenkins NA, Yazaki Y. Sequence analysis, chromosomal location, and developmental expression of the mouse preproendothelin-1 gene. Genomics. 1996; 31:177–184. [PubMed: 8824799]

Medeiros DM, Crump JG. New perspectives on pharyngeal dorsoventral patterning in development and evolution of the vertebrate jaw. Dev. Biol. 2012; 371:121–135. [PubMed: 22960284]

Miller CT, Kimmel CB. Morpholino phenocopies of *endothelin 1 sucker*) and other anterior arch class mutations. genesis. 2001; 30:186–187. [PubMed: 11477704]

Miller CT, Schilling TF, Lee K-H, Parker J, Kimmel CB. *sucker* encodes a zebrafish Endothelin-1 required for ventral pharyngeal arch development. Development. 2000; 127:3815–3838. [PubMed: 10934026]

Miller CT, Yelon D, Stainier DY, Kimmel CB. Two *endothelin 1* effectors, *hand2* and *bapx1* pattern ventral pharyngeal cartilage and the jaw joint. Development. 2003; 130:1353–1365. [PubMed: 12588851]

Moses KA, DeMayo F, Braun RM, Reecy JL, Schwartz RJ. Embryonic expression of an *Nkx2-5/Cre* gene using *ROSA26* reporter mice. genesis. 2001; 31:176–180. [PubMed: 11783008]

Nair S, Li W, Cornell R, Schilling TF. Requirements for endothelin type-A receptors and endothelin-1 signaling in the facial ectoderm for the patterning of skeletogenic neural crest cells in zebrafish. Development. 2007; 134:335–345. [PubMed: 17166927]

Nakayama K, Emoto N, Suzuki Y, Vignon-Zellweger N, Yagi K, Hirata K. Physiological relevance of hydrolysis of atrial natriuretic peptide by endothelin-converting enzyme-1. Kobe J. Med. Sci. 2012; 58:E12–E18. [PubMed: 22972025]

Pabst O, Schneider A, Brand T, Arnold HH. The mouse Nkx2-3 homeodomain gene is expressed in gut mesenchyme during pre- and postnatal mouse development. Dev. Dyn. 1997; 209:29–35. [PubMed: 9142493]

Paffett-Lugassy N, Singh R, Nevis KR, Guner-Ataman B, O'Loughlin E, Jahangiri L, Harvey RP, Burns CG, Burns CE. Heart field origin of great vessel precursors relies on *nkx2.5*-mediated vasculogenesis. Nat. Cell Biol. 2013; 15:1362–1369. [PubMed: 24161929]

Reamon-Buettner SM, Borlak J. NKX2-5: an update on this hypermutable homeodomain protein and its role in human congenital heart disease (CHD). Hum. Mutat. 2010; 31:1185–1194. [PubMed: 20725931]

Reiter JF, Alexander J, Rodaway A, Yelon D, Patient R, Holder N, Stainier DY. Gata5 is required for the development of the heart and endoderm in zebrafish. Genes Dev. 1999; 13:2983–2995. [PubMed: 10580005]

Rieder MJ, Green GE, Park SS, Stamper BD, Gordon CT, Johnson JM, Cunniff CM, Smith JD, Emery SB, Lyonnet S, et al. A human homeotic transformation tesulting from mutations in *PLCB4* and *GNAI3* causes auriculocondylar syndrome. Am. J. Hum. Genet. 2012; 90:907–914. [PubMed: 22560091]

Robu ME, Larson JD, Nasevicius A, Beiraghi S, Brenner C, Farber SA, Ekker SC. p53 activation by knockdown technologies. PLoS Genet. 2007; 3:e78. [PubMed: 17530925]

Rossi A, Kontarakis Z, Gerri C, Nolte H, Holper S, Kruger M, Stainier DY. Genetic compensation induced by deleterious mutations but not gene knockdowns. Nature. 2015; 524:230–233. [PubMed: 26168398]

Ruest L-B, Dager M, Yanagisawa H, Charité J, Hammer RE, Olson EN, Yanagisawa M, Clouthier DE. *dHAND-Cre* transgenic mice reveal specific potential functions of dHAND during craniofacial development. Dev. Biol. 2003; 257:263–277. [PubMed: 12729557]

Ruest L-B, Kedzierski R, Yanagisawa M, Clouthier DE. Deletion of the endothelin-A receptor gene within the developing mandible. Cell Tissue Res. 2005; 319:447–454. [PubMed: 15647918]

Ruest LB, Clouthier DE. Elucidating timing and function of endothelin-A receptor signaling during craniofacial development using neural crest cell-specific gene deletion and receptor antagonism. Dev. Biol. 2009; 328:94–108. [PubMed: 19185569]

Ruest LB, Xiang X, Lim KC, Levi G, Clouthier DE. Endothelin-A receptor-dependent and -independent signaling pathways in establishing mandibular identity. Development. 2004; 131:4413–4423. [PubMed: 15306564]

Sasaki MM, Nichols JT, Kimmel CB. *edn1* and *hand2* Interact in early regulation of pharyngeal arch outgrowth during zebrafish development. PLoS One. 2013; 8:e67522. [PubMed: 23826316]

Schilling, TF., Le Pabic, P. Neural crest cells in craniofacial skeletal development. In: Trainor, PA., editor. Neural Crest Cells: Evolution, Development and Disease. Elsevier; 2013. In Press

Soriano P. Generalized *lacZ* expression with the ROSA26 Cre reporter strain. Nat. Gen. 1999; 21:70–71.

Stainier DY, Kontarakis Z, Rossi A. Making sense of anti-sense data. Dev. Cell. 2015; 32:7–8. [PubMed: 25584794]

Talbot JC, Johnson SL, Kimmel CB. *hand2* and Dlx genes specify dorsal, intermediate and ventral domains within zebrafish pharyngeal arches. Development. 2010; 137:2507–2517. [PubMed: 20573696]

Tanaka M, Chen Z, Bartunkova S, Yamasaki N, Izumo S. The cardiac homeobox gene *Csx/Nkx2.5* lies genetically upstream of multiple genes essential for heart development. Development. 1999; 137:1269–1280.

Tanaka M, Schinke M, Liao HS, Yamasaki N, Izumo S. Nkx2.5 and Nkx2.6, homologs of Drosophila tinman, are required for development of the pharynx. Mol. Cell. Biol. 2001; 21:4391–4398. [PubMed: 11390666]

Tanaka M, Yamasaki N, Izumo S. Phenotypic characterization of the murine *Nkx2.6* homeobox gene by gene targeting. Mol. Cell. Biol. 2000; 20:2874–2879. [PubMed: 10733590]

Targoff KL, Colombo S, George V, Schell T, Kim SH, Solnica-Krezel L, Yelon D. Nkx genes are essential for maintenance of ventricular identity. Development. 2013; 140:4203–4213. [PubMed: 24026123]

Targoff KL, Schell T, Yelon D. Nkx genes regulate heart tube extension and exert differential effects on ventricular and atrial cell numbe. Dev. Biol. 2008; 322:314–321. [PubMed: 18718462]

Tavares ALP, Garcia EL, Kuhn K, Woods CM, Williams T, Clouthier DE. Ectodermal-derived Endothelin1 is required for patterning the distal and intermediate domains of the mouse mandibular arch. Dev. Biol. 2012; 371:47–56. [PubMed: 22902530]

Trainor PA, Krumlauf R. Hox genes, neural crest cells and branchial arch patterning. Curr. Opin. Cell. Biol. 2001; 13:698–705. [PubMed: 11698185]

Tu CT, Yang TC, Tsai HJ. Nkx2.7 and Nkx2.5 function redundantly and are required for cardiac morphogenesis of zebrafish embryos. PLoS One. 2009; 4:e4249. [PubMed: 19158954]

Vieux-Rochas M, Mantero S, Heude E, Barbieri O, Astigiano S, Couly G, Kurihara H, Levi G, Merlo GR. Spatio-temporal dynamics of gene expression of the Edn1-Dlx5/6 pathway during development of the lower jaw. genesis. 2010; 48:262–373. [PubMed: 20333701]

Walker M, Kimmel CB. A two-color acid-free cartilage and bone stain for zebrafish larvae. Biotech. Histochem. 2007; 82:23–28. [PubMed: 17510811]

Walker MB, Miller CT, Swartz ME, Eberhart JK, Kimmel CB. *phospholipase C, beta 3* is required for Endothelin1 regulation of pharyngeal arch patterning in zebrafish. Dev. Biol. 2007; 304:194–207. [PubMed: 17239364]

Walker MB, Miller CT, Talbot JC, Stock DW, Kimmel CB. Zebrafish *furin* mutants reveal intricacies in regulating Endothelin1 signaling in craniofacial patterning. Dev. Biol. 2006; 295:194–205. [PubMed: 16678149]

Westerfield, M. The Zebrafish Book: A guide for the laboratory use of zebrafish (Danio rerio). 4th. Eugene: University of Oregon Press; 1993.

Xu D, Emoto N, Giaid A, Slaughter C, Kaw S, deWit D, Yanagisawa M. ECE-1: a membrane-bound metalloprotease that catalyzes the proteolytic activation of big endothelin-1. Cell. 1994; 78:473–485. [PubMed: 8062389]

Yanagisawa H, Hammer RE, Richardson JA, Emoto N, Williams SC, Takeda S, Clouthier DE, Yanagisawa M. Disruption of *ECE-1* and *ECE-2* reveals a role for endothelin-converting enzyme-2 in murine cardiac development. J. Clin. Invest. 2000; 105:1373–1382. [PubMed: 10811845]

Yanagisawa H, Yanagisawa M, Kapur RP, Richardson JA, Williams SC, Clouthier DE, de Wit D, Emoto N, Hammer RE. Dual genetic pathways of endothelin-mediated intercellular signaling revealed by targeted disruption of endothelin converting enzyme-1 gene. Development. 1998; 125:825–836. [PubMed: 9449665]

Yanagisawa M. The endothelin system: a new target for therapeutic intervention. Circulation. 1994; 89:1320–1322. [PubMed: 8124823]

Yanagisawa M, Kurihara H, Kimura S, Tomobe Y, Kobayashi M, Mitsui Y, Yazaki Y, Goto K, Masaki T. A novel potent vasoconstrictor peptide produced by vascular endothelial cells. Nature. 1988; 332:411–415. [PubMed: 2451132]

Yu W, Hegarty JP, Berg A, Chen X, West G, Kelly AA, Wang Y, Poritz LS, Koltun WA, Lin Z. *NKX2-3* transcriptional regulation of endothelin-1 and VEGF signaling in human intestinal microvascular endothelial cells. PLoS One. 2011; 6:e20454. [PubMed: 21637825]

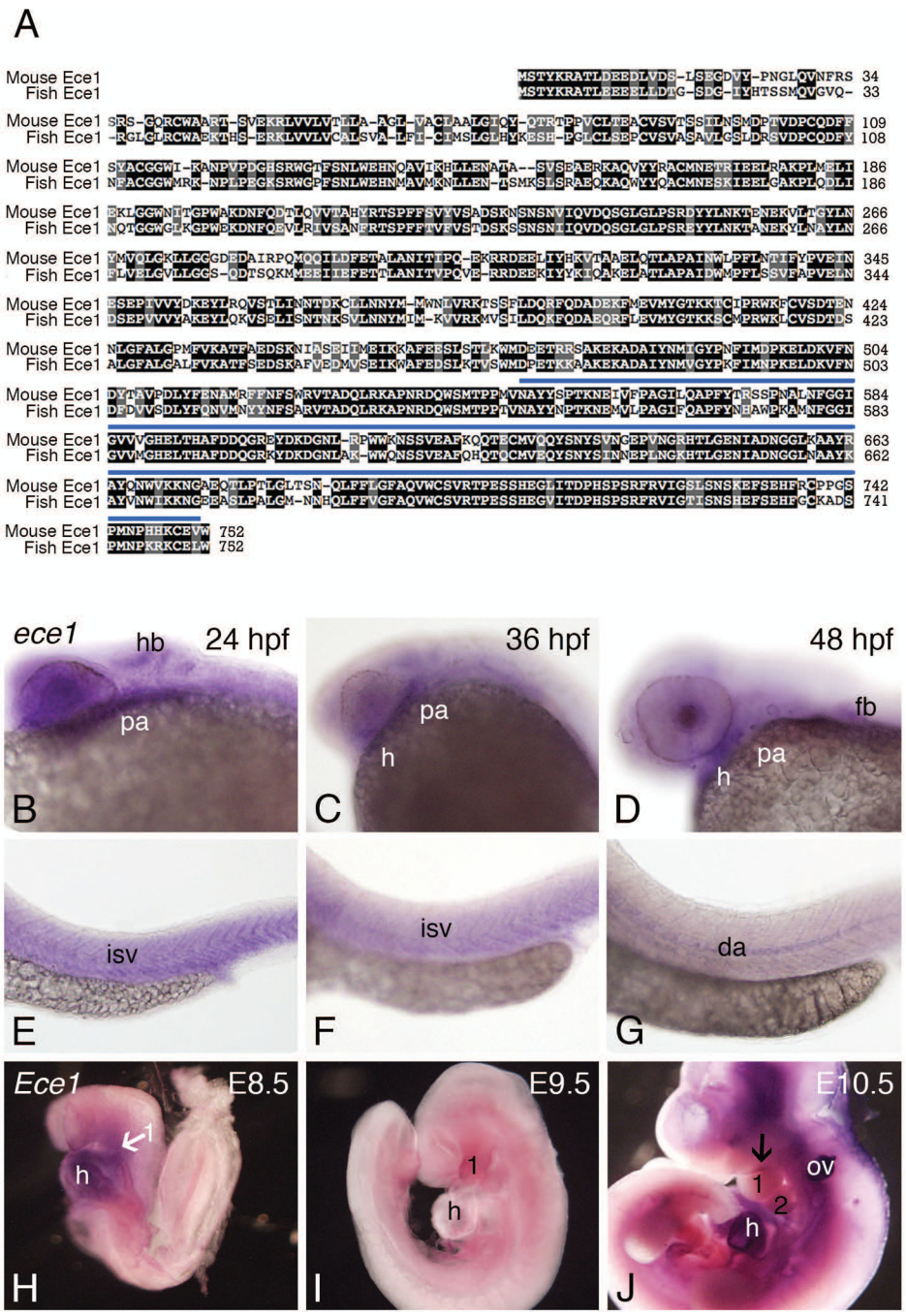

Figure 1. Analysis of zebrafish *ece1* sequence and expression

A. Amino acid alignment between fish and mouse Ece1. Identical amino acids are indicated with a black background, similar amino acids indicated with a gray background, and the C-terminal peptidase region indicated with an overlying blue line. **B–G.** *ece1* expression in the developing zebrafish. At 24 hpf, *ece1* expression is observed in the hindbrain (hb), pharyngeal arches (pa), somites and intersegmental vessels (isv) (B, E). At 36 hpf, *ece1* expression is more concentrated in the anterior arches, with expression also in somites and intersegmental vessel (C, F). At 48 hpf, *ece1* is detectable in the heart and fin bud (fb) in

addition to being broadly expressed throughout the embryo (D), including the dorsal aorta (G). **H–J.** *Ece1* expression in the developing mouse is observed in the head, heart (h) and mandibular portion of arch one (1) at E8.5 (H). By E9.5, strong *Ece1* expression is only observed in the mandibular portion of the first arch (1)(I). At E10.5, *Ece1* expression is observed in the maxillary portion of the first arch (arrow), heart, and otic vessel (ov)(J). 2, second pharyngeal arch.

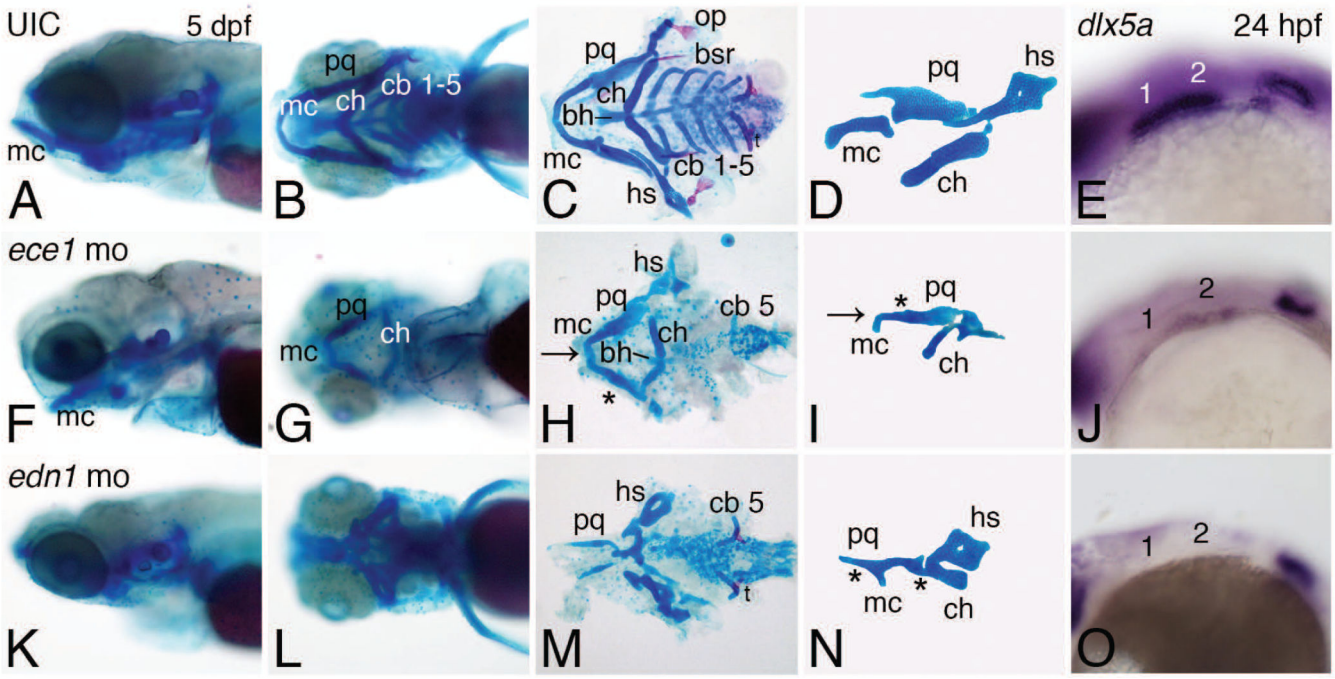

Figure 2. *ece1* knockdown leads to defects in craniofacial cartilage development

Analysis of 5 dpf uninjected control (UIC) embryos (A–D), *ece1* (F–I) and *edn1* (K-N) morphants and 24 hpf control (E) or morphant (J, O) embryos after ISH to examine *dlx5a* expression (shown in lateral orientation. Embryos are shown in gross lateral (A, E, F, J, K, O), gross ventral (B, G, L), flat mount ventral (C, H, M) and flat mount lateral (D, I, N) orientation. **A–D.** Control embryos. **E.** Whole mount ISH showing normal *dlx5a* expression in the first (1) and second (2) pharyngeal arches. **F–I.** *ece1* morphants show defects in the ventral and dorsal viscerocranial elements, including a downward defection of Meckel's cartilage (mc) (arrows in H and I) and a fusion between Meckel's and the palatoquadrate (pq)(asterisk) (H, I) The ceratohyal (ch) is also defected downward and smaller, as is the basihyal (bh). **J.** *dlx5a* expression is downregulated in arches one and two in *ece1* morphants. **K–N.** In *edn1* morphants, there is a reduction in ventral cartilages and loss of joints. This includes a severely downturned Meckel's cartilage (mc) that is fused with the palatoquadrate (asterisk in N). The ceratohyal is also pulled ventrally and fused with hyomandibular region, with the symplectic region of the hyosymplectic absent (*)(N). Only the fifth ceratobranchial containing the pharyngeal teeth (t) are present (N). **O.** *dlx5a* expression is completely downregulated in arches one and two in *edn1* morphants. cb 1–5, ceratobranchials 1–5; bsr, branchiostegal rays; op, opercle.

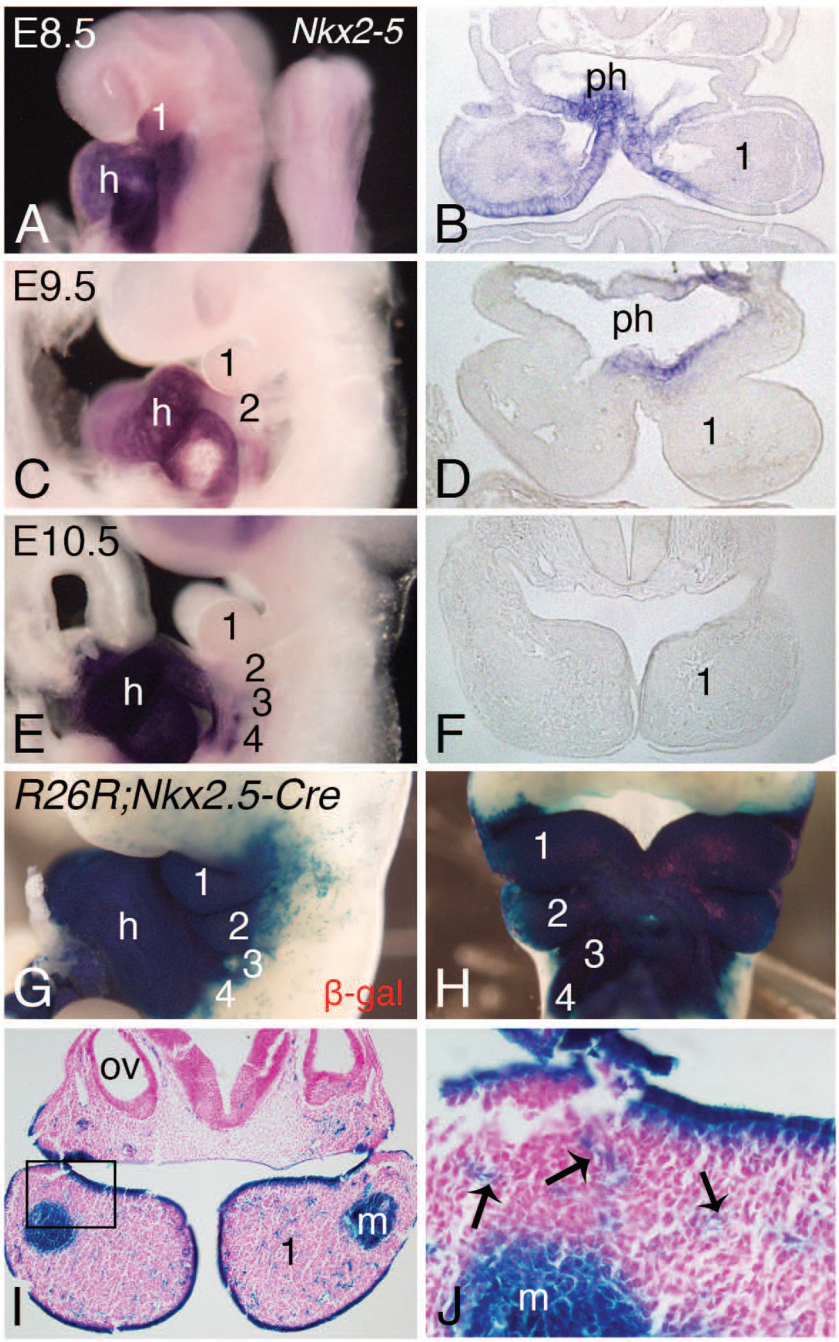

Figure 3. ***Nkx2-5*** **expression and fate of** ***Nkx2-5*** **daughter cells in the mouse embryo**

A–F. Analysis of stained embryos following whole mount ISH (A, C, E) and following transverse sectioning of stained embryos (B, D, F). **A, B.** In E8.5 control embryos, *Nkx2-5* expression in observed in the heart (h) and ectoderm of the first pharyngeal arch (1) and pharynx (ph), with scattered staining present in the first arch mesenchyme. **C, D.** In E9.5 embryos, *Nkx2-5* is strongly expressed in the heart and pharynx, but arch expression is lost. **E, F.** By E10.5, *Nkx2-5* expression is only observed in the heart. **G–J.** β-galactosidase (β-gal) staining in E10.5 *R26R;Nkx2-5-Cre* embryos. Strong staining (representing Nkx2-5

daughter cells) is observed throughout the ectoderm of the pharyngeal arches and in the heart. Sections through the mandibular arch (1) show β-gal staining in the pharyngeal arch ectoderm, endoderm and mesodermal core (m) (I, J). Higher magnification shows that the β-gal staining is present in the developing vasculature (arrows in J), while the NCC-derived mesenchyme is unstained. 1–4, pharyngeal arches 1–4; ov, otic vesicle.

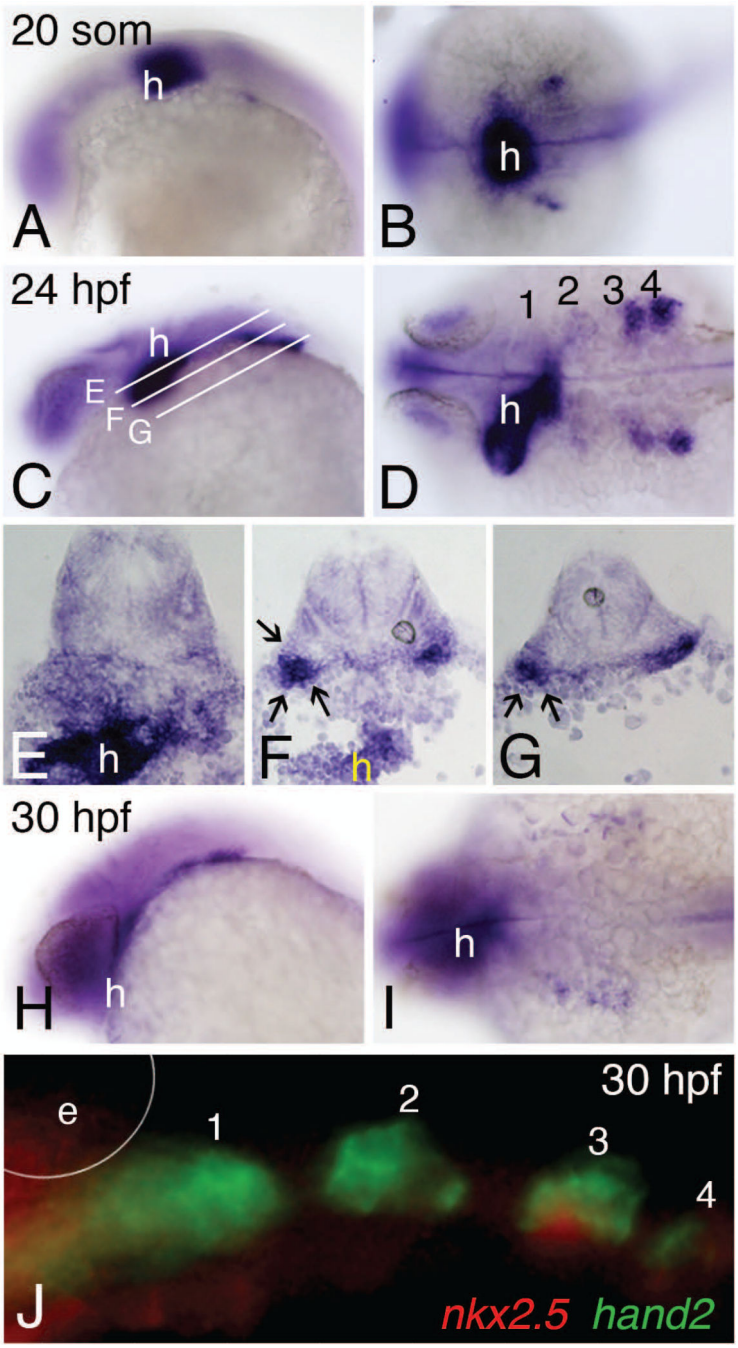

Figure 4. *nkx2.5* expression in the heart and early pharyngeal arch ectoderm in fish

A, B. Lateral and dorsal views of a 20 somite zebrafish embryo showing strong expression along the midline in the developing heart (h) as well as more lateral expression domains in the developing pharyngeal arches. **C, D.** At 24 hpf, expression continues in the heart and pharyngeal arches 1–4, though expression in arch 1 is barely visible. **E–G.** Transverse sections through the stained embryo shown in panel C along the planes indicated. Stained cells are between the ectoderm and underlying endoderm, likely corresponding to the arch mesoderm (arrows in F and G). **H, I.** *nkx2.5* expression persists through 30 hpf, although the

expression in the arch mesoderm is decreased. **J.** Lateral view following double fluorescent ISH for *nkx2.5* (red) and *hand2* (green) in 30 hpf zebrafish embryo. *nkx2.5* is localized in the arch mesoderm medial to NCCs, labeled by *hand2*. Both *nkx2.5* and *hand2* are expressed in the heart at this stage.

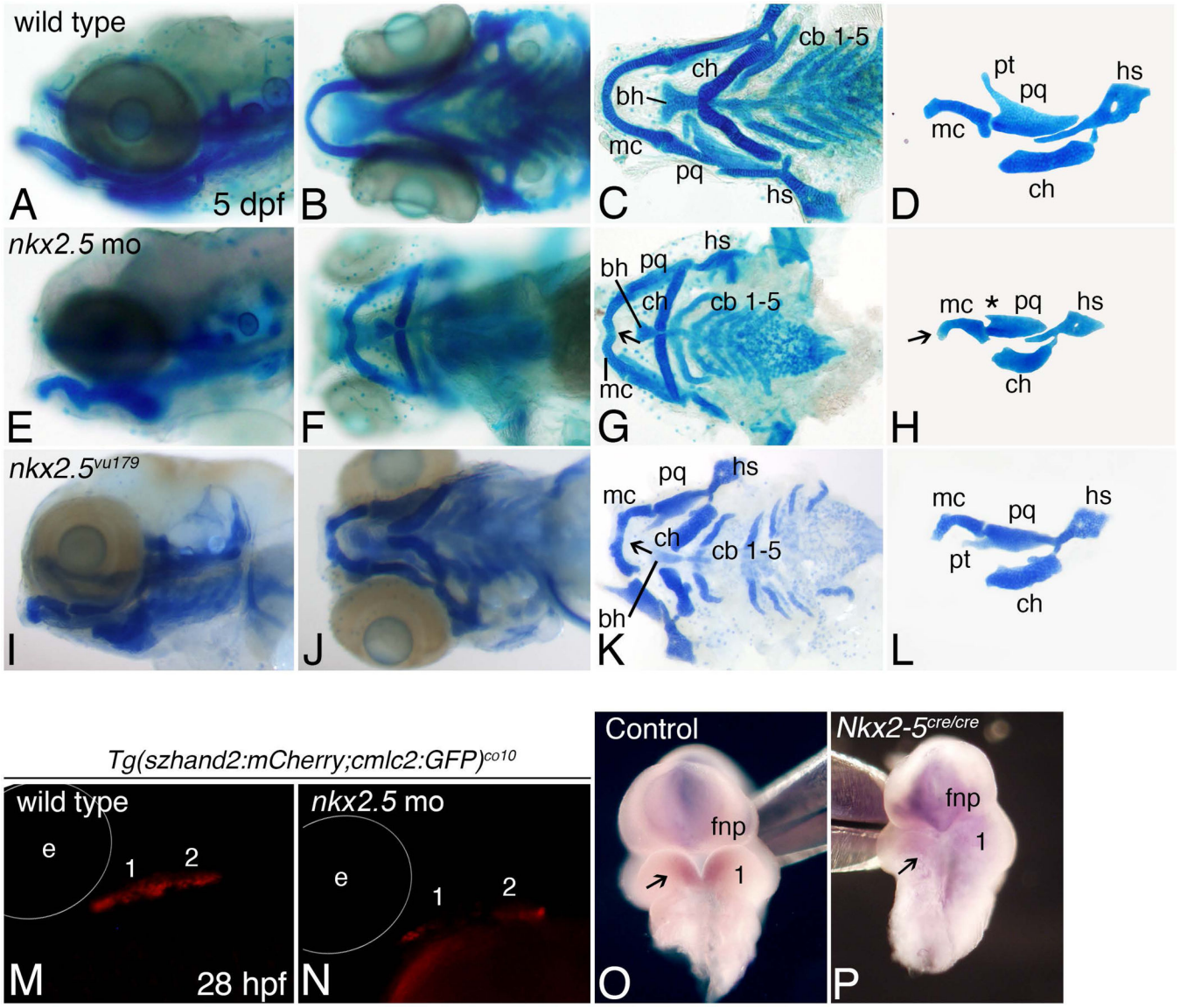

Figure 5. Reduction or loss of *nkx2.5* leads to viscerocranial cartilage defects

A–L. 5 dpf zebrafish embryos stained with Alcian blue to visualize cartilage and shown in lateral (A, E, I), ventral (B, F, J), ventral flat mount (C, G, K) and lateral flat mount (D, H, L) views. **A–D.** Uninjected control (UIC) embryos. **E–H.** In *nkx2.5* morphants, Meckel's cartilage (mc) is shortened, downturned at the tip (E, arrows in G, H) and is fused with the palatoquadrate (pq)(H). The pterygoid process (pt) of the palatoquadrate is truncated (asterisk in H). Other cartilages are hypoplastic, including ceratobranchial cartilages 1–5 (cb 1–5 in G) and the basihyal (bh) (G). **I–L.** In *nkx2.5*^{vu179} mutants, Meckel's cartilage is hypoplastic and the tip is downturned (I, L and arrow in K). The ceratohyal (ch) is also hypoplastic (L), though is larger than that observed in *nkx2.5* morphants (H). The ceratobranchial cartilages, hyosymplectic (hy), basihyal and the palatoquadrate are also smaller, though the pterygoid process of the palatoquadrate is present (L) (the downward angle of the pterygoid process is due to the mounting angle). **M, N.** In *szhand2:mcherry*

transgenic zebrafish, mCherry fluorescence is driven in the pharyngeal arches by the zebrafish *hand2* pharyngeal arch enhancer (M). In *nkx2.5* morphants, fluorescence is reduced (N). **O, P**. Expression of *Hand2* in the mandibular arch of E9.5 control embryos (O) is absent the mandibular arch of E9.5 *Nkx2-5*$^{cre/cre}$ embryos (P).

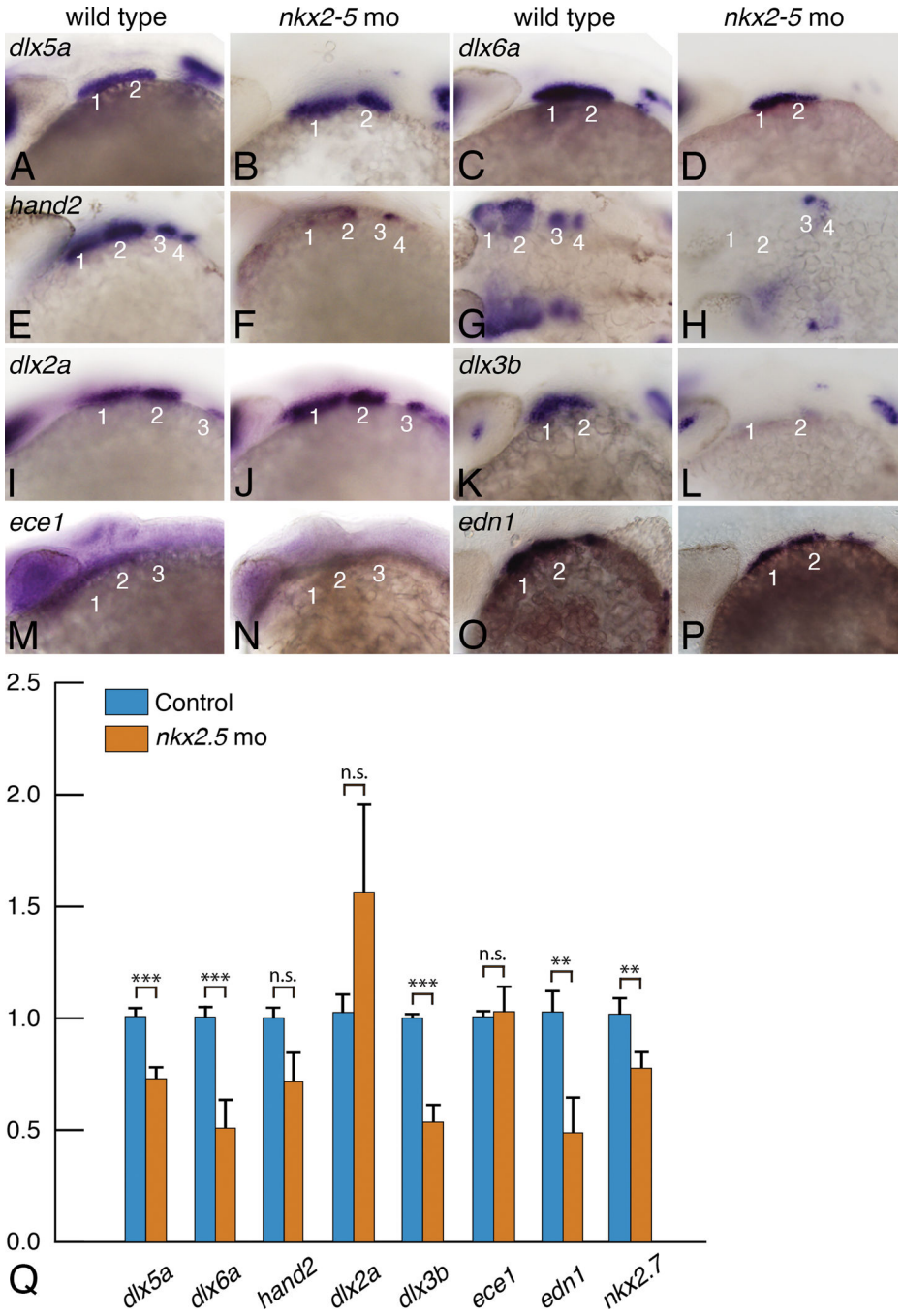

Figure 6. Gene expression changes in 24 hpf *nkx2.5* morphants

A, B. *dlx5a* expression appears unchanged in morphant embryos (B) compared to expression levels in wild type embryos (A). **C, D.** *dlx6a* expression is partially downregulated in morphants (D). **E–H.** *hand2* expression in morphants is almost completely lost except for small domains remaining in arches 3 and 4 (F, H). **I, J.** Arch expression of *dlx2a* appears unchanged or slightly increased in morphants (J) compared to that observed in wild type embryos (I). **K, L.** *dlx3b* expression is essentially lost in the pharyngeal arches of morphants (L). **M, N.** Expression of *ece1* in the pharyngeal arches appears decreased in morphants (N).

O, P. Arch expression of *edn1* is decreased in *nkx2.5* morphants (P) compared to control embryos (O). **Q.** qRT-PCR analysis of gene expression in 24 hpf control (blue bars) and *nkx2.5* MO (orange bars) larvae. Analysis was performed on embryos obtained from three separate morpholino injection experiments, with 40–50 whole embryos from each experiment used for RNA collection. n.s., not significant; *, $p \leq 0.05$; **, $p \leq 0.01$; ***, $p \leq 0.005$.

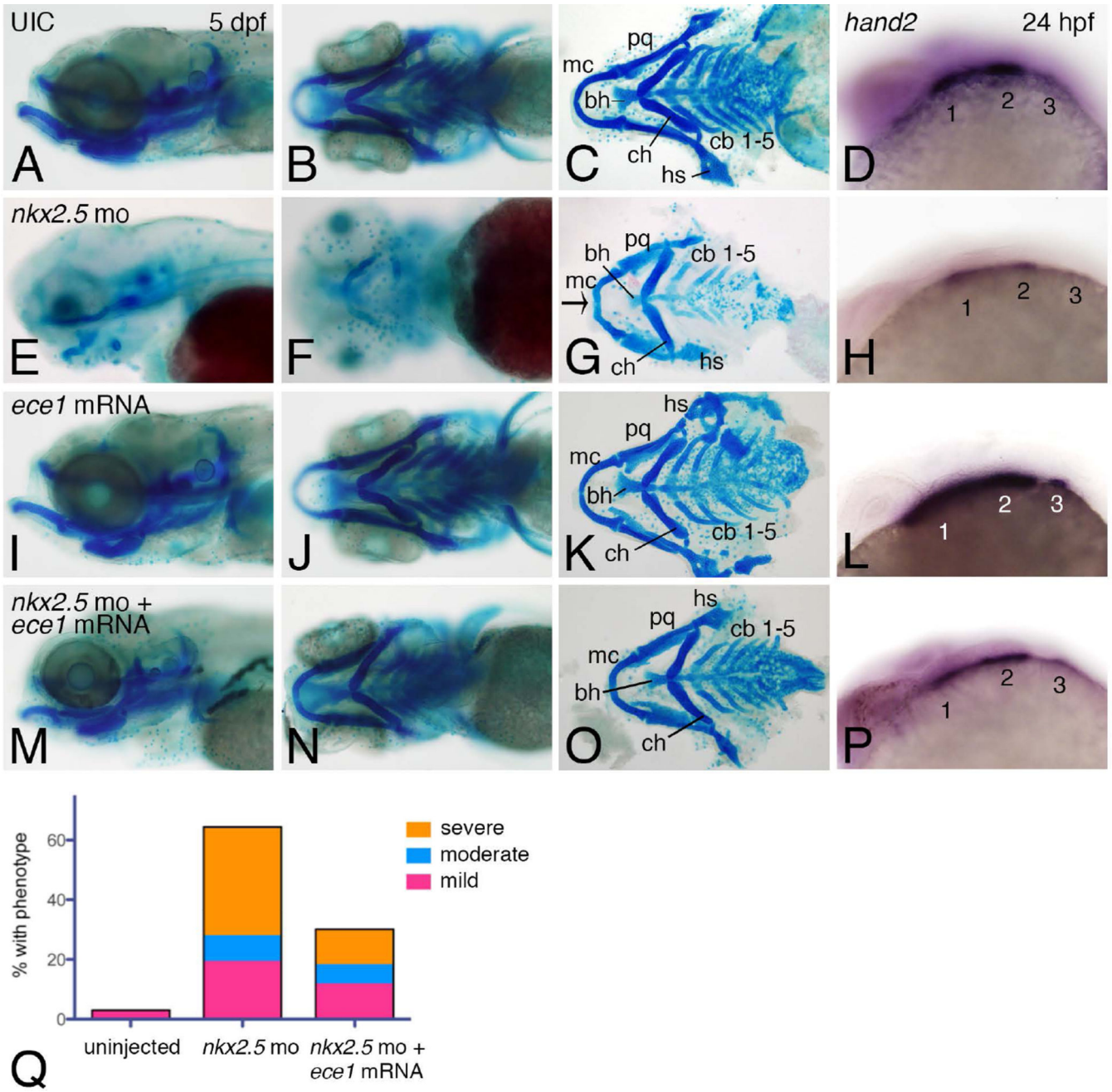

Figure 7. *ece1* mRNA rescues the *nkx2.5* morphant phenotype

5 dpf embryos stained with Alcian blue and shown in lateral (A, E, I, M), ventral (B, F, J, N) and ventral flat mount (C, G, K, O) orientation and 24 hpf embryos after ISH to examine *hand2* expression (shown in lateral orientation (D, H, L, P). **A–D.** Uninjected control (UIC) embryos. **E–H.** In *nkx2.5* morphants, the entire viscerocranium is hypoplastic, with Meckel's cartilage (mc) showing a downward deflection at the tip (arrow in G) and almost complete loss of *hand2* expression (H). **I–L.** Injection of *ece1* mRNA into wild type embryos does not affect cartilage structures (I–K) or *hand2* expression (L). **M–P.** Embryos co-injected with *ece1* mRNA and *nkx2.5* MO have relatively normal cartilage structures at 5

dpf (M–O) while *hand2* expression is partially rescued at 24 hpf (P). **Q.** Quantification of morphant phenotype rescue by *ece1* mRNA. bh, basihyal, cb1-5, ceratobranchials 1–5; ch, ceratohyal; hs, hyosymplectic; mc, Meckel's cartilage; pq, palatoquadrate; 1, 2, 3, pharyngeal arches 1–3.